A shallow water model for the numerical simulation of overland flow on surfaces with ridges and furrows

Ulrich Razafison, Stephane Cordier, Olivier Delestre, Frédéric Darboux, Carine Lucas, Francois James

A shallow water model for the numerical simulation of overland flow on surfaces with ridges and furrows

Ulrich Razafison[1], Stéphane Cordier[2], Olivier Delestre[2], Frédéric Darboux[3], Carine Lucas[2] and François James[2]

1 - Université de Franche-Comté, Laboratoire de Mathématiques, CNRS UMR 6623, 16 route de Gray, 25030 Besançon Cedex, France

2 - Université d'Orléans, Laboratoire MAPMO, CNRS UMR 6628, Fédération Denis-Poisson, FR CNRS 2964, B. P. 6759, 45067 Orléans Cedex 2, France

3 - INRA, UR 0272 Science du sol, Centre de recherche d'Orléans, CS 40001, F-45075 Orléans Cedex 2, France

Email adresses: *ulrich.razafison@math.cnrs.fr, stephane.cordier@univ-orleans.fr, olivierdelestre41@yahoo.fr, frederic.darboux@orleans.inra.fr, francois.james@univ-orleans.fr, carine.lucas@univ-orleans.fr,*

Abstract

We introduce here a new shallow water model for the numerical simulation of overland flow with furrows effects without representing them explicitly. The model is obtained by adding to the classical shallow water equations a friction term that takes into account these effects.

We validate the model with some numerical tests and we present comparisons with simulations computed with the classical shallow water model where the furrows are explicitly described.

Keywords: Overland flow, Shallow water equations, Furrows, Friction

AMS Classification: 93A30, 81T80, 58J45, 35L65

1 Introduction

During rainfalls, overland flow on cultivated lands induces problems at watershed scale for soil conservation (decrease of soil thickness by erosion, nutrient losses), infrastructure (flooding and destruction of roads and buildings), preservation of water quality (drinking water) and sustainability of aquatic ecosystems (chemical pollution).

These troubles can be prevented by watershed management. Improving watershed management in relationships with overland flow requires to have a good prediction of the

water flux at the watershed outlet but also a good prediction of the spatial distribution of flux over the whole watershed. However, the current hydrological models are inefficient in predicting overland flow within small watersheds (see [4, 15, 16]). In agricultural watersheds, one of the main difficulties is that flow directions are controlled not only by the topography, but also, on field boundaries, by ditches along the fields, and, inside the fields, by ridges and furrows created by tillage operations. The flow pattern is clearly the result of the interaction between these objects [22], but the way they interact remains mostly unspecified. Therefore, one must improve the understanding of this interaction in order to better predict the spatial and temporal distribution of overland flow and so to improve the decisions made by watershed managers.

In this paper we focus on the interaction between topography and furrows because it is a very common case, encountered in almost all cultivated lands. This interaction can be seen as the interaction between three types of roughness. The topography is the roughness of the Earth and is described in Digital Elevation Maps with a horizontal resolution larger than one meter, and commonly of ten meters and more. The furrows are the roughness due to agricultural practices and create a strong directional heterogeneity inside a field. They are characterized by their wavelength (of about one to a few decimeters), their amplitude (of a few centimeters to one decimeter) and their direction. Finally the random roughness, due to soil aggregates and clods, is homogeneous in direction and has an amplitude of a few millimeters to about one decimeter. To our knowledge, most of the works on the interaction between roughness and flow have been dedicated to topography (see [21] and [24]) or to random roughness (see [8], [17] and [14]).

Few works are dealing with furrows, and among them, most are concerned with the storage capacity of the furrows, i.e. the amount of water stored in the puddles created by the furrows (for instance [20]). So, these works do not consider the water flowing on the soil surfaces but only the water stored in puddles. The few works considering both overland flow and the furrows-topography interaction are empirical studies [22, 23]. They lead to empirical laws giving an on/off prediction: the predicted flow direction is either the direction of the topographic slope or the furrow direction, while in reality water can flow in both directions at the same time. Moreover, these laws are limited by their empirical basis.

To be of practical use, a model accounting for the effects of furrows on overland flow direction must not require an explicit representation of the furrows: that would imply the use of a digital map with a horizontal resolution of about a centimeter for the whole watershed, which has as typical size of a square kilometer for the small ones. Such digital maps are not available and, even if available, will require to much computation resources. The purpose of this work is to propose a model that is able to take into account the effects

of the furrows on overland flow and to present the numerical results we obtained. The model is a first step in an attempt to predict overland flow directions controlled by furrows and topography without representing the furrows explicitly. Indeed, the furrows are known only trough their average amplitude, their average wavelength and their direction. At the current stage, furrow direction is kept perpendicular to the slope. Our model is based on the so-called shallow water equations that are widely used to describe flows in rivers, in ocean and overland flow among other applications.

The outline of the paper is as follow. In the next section, we present the model that we propose to account for the effects of the furrows on overland flow. In section 3, we present and discuss the numerical results that we obtain with our model. Conclusions are outlined in Section 4.

2 The mathematical models

The starting point is the 2D classic shallow water system [9] in a bounded domain Ω:

$$\begin{cases} \dfrac{\partial h}{\partial t} + \dfrac{\partial hu}{\partial x} + \dfrac{\partial hv}{\partial y} = R, \\ \dfrac{\partial hu}{\partial t} + \dfrac{\partial hu^2}{\partial x} + \dfrac{\partial huv}{\partial y} + gh\dfrac{\partial h}{\partial x} + gh\dfrac{\partial Z}{\partial x} + gk^2h^{-1/3}|\boldsymbol{u}|u = 0, \\ \dfrac{\partial hv}{\partial t} + \dfrac{\partial huv}{\partial x} + \dfrac{\partial hv^2}{\partial y} + gh\dfrac{\partial h}{\partial y} + gh\dfrac{\partial Z}{\partial y} + gk^2h^{-1/3}|\boldsymbol{u}|v = 0, \end{cases} \tag{2.1}$$

where $t > 0$ and $\boldsymbol{x} = (x, y) \in \Omega$. The unknowns are the water height $h = h(t, \boldsymbol{x})$ and the horizontal flow velocity $\boldsymbol{u} = \boldsymbol{u}(t, \boldsymbol{x}) = (u(t, \boldsymbol{x}), v(t, \boldsymbol{x}))^T$. Furthermore, g is the acceleration due to the gravity, R is the rainfall intensity and $Z(\boldsymbol{x})$ describes the bottom topography of the domain and therefore $h + Z$ is the level of the water surface (see Figure 1). We denote also $\boldsymbol{q}(t, \boldsymbol{x}) = (q_x(t, \boldsymbol{x}), q_y(t, \boldsymbol{x}))^T = h(t, \boldsymbol{x})\boldsymbol{u}(t, \boldsymbol{x})$ the flux of water. For the friction term, we here use the Manning's law with k the Manning's coefficient. We refer for instance to [12, 13, 19] for a derivation of the shallow water system departing from the free surface Navier-Stokes equations.

We now consider a rectangular domain Ω and a topography Z with furrows. We suppose that the topography has a constant slope and that the geometry of the furrows is known through their average amplitude and their average wavelength. We also suppose that the furrows are perpendicular to the length of Ω. An example of such a topography is illustrated in Figure 2.

Next, we shall complete the problem with the following assumptions.

1. The direction of the flow is parallel to the length of the domain Ω.
2. We only consider fluvial flows which means that $|\boldsymbol{u}| < \sqrt{gh}$.

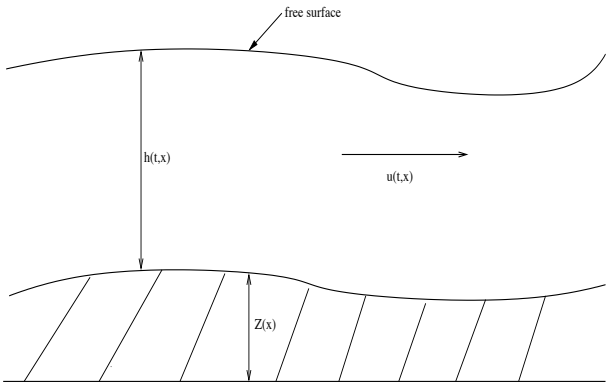

Figure 1: A 1D shallow water flow

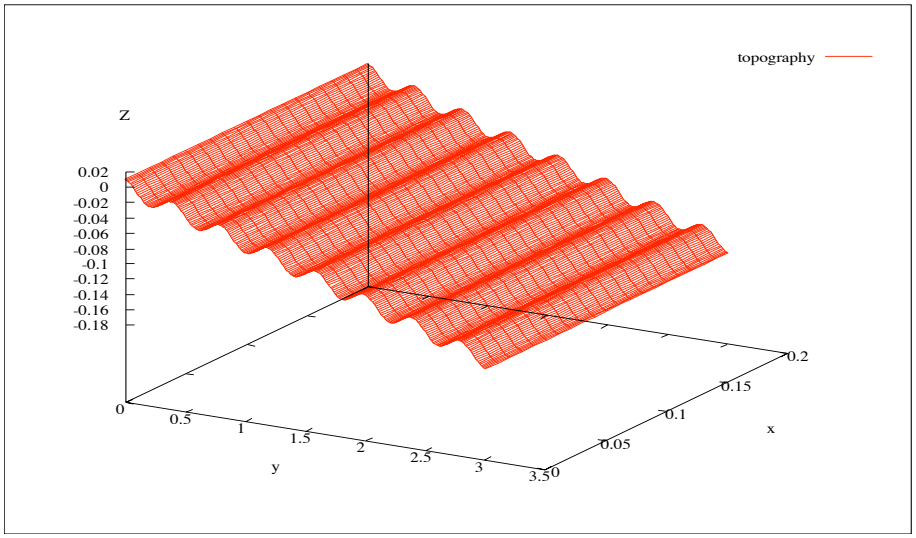

Figure 2: An example of a topography with furrows that we consider

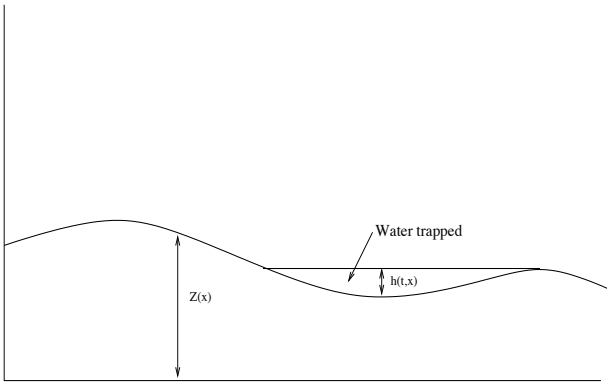

Figure 3: Water trapped in a furrow

3. Infiltration and soil erosion are not taken into account.

Under such assumptions, the furrows overflow at the same time during rainfall events or one by one in the case of inflow from upstream.

We aim to propose a model that takes into account the effects of the furrows without explicitly representing them in the topography Z. In other words, we want to find an equivalent model to the shallow water system on Ω, that would be used on a topography which is an inclined plane. We want to force the flow to slow down when the flow depth is smaller than the furrow average amplitude. Furthermore, we want this effect caused by the furrows be modelled through an additional friction term that forces the flow to slow down for small flow depth. To that end, we first introduce $\langle h \rangle$ the average height of the water trapped in the furrows (see Figure 3), that only depends on the slope of the domain, on the furrows average amplitude and on the furrows average wavelength. We next consider the following additional friction coefficient:

$$K(h) = K_0 \, e^{\left(\frac{-h+\langle h \rangle}{C\langle h \rangle}\right)}, \tag{2.2}$$

where C is a characteristic constant related to the height variations of the furrows and K_0 is a coefficient. In Figure 4, the general shape of $K(h)$ is plotted for $\langle h \rangle = 0.01$ m. We clearly see that $K(h)$ is large for $h \leq \langle h \rangle$. This shows that when the water height h is lower than the average height of the furrows $\langle h \rangle$ then, thanks to $K(h)$, the flow is slowed down.

Remark 2.1. 1. If $\langle h \rangle$ tends to 0, then $K(h)$ also tends to 0 for any $h > 0$. In other words, the additional friction coefficient disappears when there are no furrows.

2. If C tends to 0, then we obtain the empirical models, giving an on/off prediction of the furrows-topography interaction (see [22, 23]). The new shallow water model

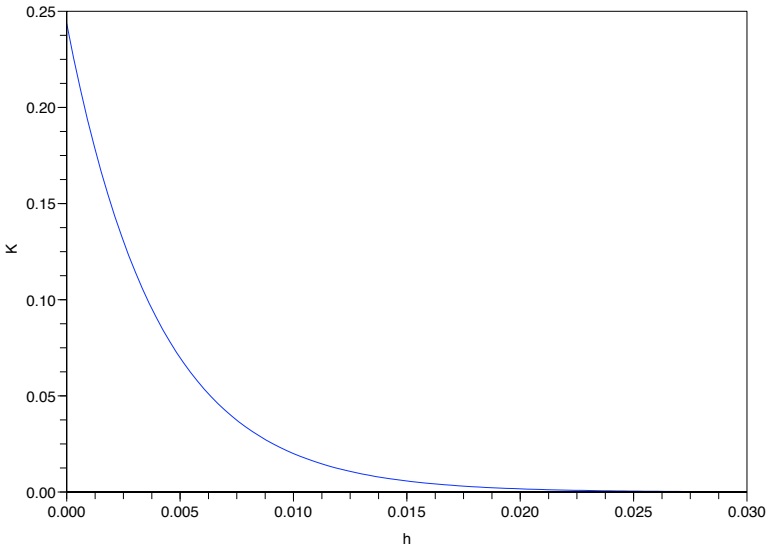

Figure 4: A shape of the friction term $K(h)$

that we propose (see (2.3)) can then be seen as a generalisation of these models.

3. The constant C may also be related to the random variations of the amplitudes of the furrows. The validation of this assumption is in progress in the two-dimensional extension of this work.

Finally, we propose the following new shallow water model:

$$\begin{cases} \dfrac{\partial h}{\partial t} + \dfrac{\partial hu}{\partial x} + \dfrac{\partial hv}{\partial y} = R, \\ \dfrac{\partial hu}{\partial t} + \dfrac{\partial hu^2}{\partial x} + \dfrac{\partial huv}{\partial y} + gh\dfrac{\partial h}{\partial x} + gh\dfrac{\partial Z}{\partial x} + gk^2h^{-1/3}|\boldsymbol{u}|u = 0, \\ \dfrac{\partial hv}{\partial t} + \dfrac{\partial huv}{\partial x} + \dfrac{\partial hv^2}{\partial y} + gh\dfrac{\partial h}{\partial y} + gh\dfrac{\partial Z}{\partial y} + gk^2h^{-1/3}|\boldsymbol{u}|v + K(h)hv = 0. \end{cases} \tag{2.3}$$

Remark 2.2. 1. Note that, since the direction of the furrows are perpendicular to the slope, the additional friction law $K(h)hv$ only appears in the third equation of (2.3) and therefore, it only acts on the flow in the y-axis direction. In general, the direction of the furrows is constant on a cell grid over the area of agricultural fields. If this direction is not perpendicular to the slope, then the equations can be obtained by rotation.

2. The friction law in the new model is arbitrarily chosen. It is a particular case of the more general friction law that we have considered which is of the form $K(h)h^\alpha|\boldsymbol{u}|^\beta v$

where α and β are positive real numbers. In (2.3), we have $(\alpha, \beta) = (1, 0)$. For the numerical test cases that we have considered in this work (see the next section), we have also performed simulations with the following values $(\alpha, \beta) = (1, 1)$ and $(\alpha, \beta) = (-1/3, 1)$. These simulations lead to similar results than the ones of $(\alpha, \beta) = (1, 0)$.

At this point, let us mention that, since shallow water flows can also be described by the so-called multi-layer shallow water system (see for instance to [1], [3], [7] and references therein for a derivation and numerical studies), we can propose another approach based on multi-layer models to take into account the effects of the furrows on overland flows. In this work, we introduce the following two-layer like model:

$$\begin{cases} \text{if } h(t, \boldsymbol{x}) \leq \langle h \rangle, \text{ then } \boldsymbol{u}(t, \boldsymbol{x}) = \mathbf{0} \text{ and } h(t, \boldsymbol{x}) = Rt, \\ \\ \text{if } h(t, \boldsymbol{x}) > \langle h \rangle, \text{ then solve (2.1) where the topography is an inclined plane.} \end{cases} \tag{2.4}$$

In (2.4), the lower layer corresponds to the filling up of the furrows; note that the upper layer is active only when the furrows overflow. The initial conditions for the upper layer are then $\boldsymbol{u}(0, \boldsymbol{x}) = \mathbf{0}$ and $h(0, \boldsymbol{x}) = \hat{h} - \langle h \rangle$, where $\hat{h}$ is the water height at the overflow time. Note that, this model provides more satisfactory results than the model (2.3) (see the next section). But its extension to more complex two-dimensional problems, requires a careful modelling of the coupling between the two layers and it is more difficult than the extension of the model (2.3). This work is in progress in our project.

3 Numerical results

In this section, we present two test cases in order to illustrate the ability of the new model (2.3) to take into account the effects of the furrows. We compare it with the shallow water model (2.1) where the furrows are removed from the topography. The first test case is with water input from rainfall. For this test, we also present the results obtained with the two-layer like model (2.4). The second test case is with water input from upstream. In both test cases, we consider as reference solutions the ones obtained from the shallow water model (2.1) where the geometry of the furrows is known explicitly. We briefly mention that the numerical approximation is based on finite volume methods for hyperbolic system of conservation laws. In particular, we use well-balanced schemes with hydrostatic reconstruction developed in [2, 5] and, following [6], we introduce a semi-implicit treatment of the Manning friction term. Concerning the treatment of the boundary conditions, we follow the ideas developed in [6] (see also [18]). For a detailed description of the numerical method in the context of overland flow on agricultural fields, we refer to [10] and [11]. All the numerical results are obtained using the C++ software

FullSWOF (Full Shallow Water equations for Overland Flow) developed at the MAPMO lab., University of Orléans, France.
We consider a domain Ω of length $L = 4$ m and of width $\ell = 0.2$ m. The length of Ω is parallel to the y-axis (see Figure 2). We assume that the topography Z has a constant slope of 5%. The average amplitude of the furrows is 0.02 m and their average wavelength is 0.1 m. We choose a friction coefficient $k = 0.04\ \mathrm{m}^{\frac{1}{3}}\ \mathrm{s}^{-1}$. For the following computations, we use a time step $\Delta t = 0.001$ s.

3.1 Computing reference solutions

This paragraph is devoted to the computation of the solutions of the shallow water model (2.1) where the geometry of the furrows is known explicitly. These solutions will be considered here as reference solutions. According to the parameters given above, the topography is modelized by the equation:

$$Z(x, y) = -0.05\, y + 0.01 \cos(20\pi\, y). \tag{3.5}$$

The domain is discretized by a mesh with $8,000$ rectangles. The length and the width of the domain are discretized with a space step equal to 0.01 m. This means that in each furrow we have 200 cells. We assume that the domain is initially empty which implies that $\boldsymbol{u}(0, \boldsymbol{x}) = \mathbf{0}$ and $h(0, \boldsymbol{x}) = 0$.

3.1.1 Rainfall test case

In this case, we assume rainfall on the domain with a constant permanent rain intensity $R = 8\text{E}{-}04$ m s^{-1}. The rain discharge is then $Q_R = 6.4\text{E}{-}04$ m^3 s^{-1}. The final time is $T = 22.5$ s. Note that, since we are interested in the effects of the furrows, we focus on the transitional stage of the flow. Therefore the final time T is chosen such that the outflow discharge is approximately equal to the half of the rain discharge. We assume here that at the upstream of the domain there is a solid wall. We show in Figure 5 the side-view of the water height at the final time.

3.1.2 Inflow test case

We now consider a permanent inflow from upstream. We prescribe $Q_I = 1.566\text{E}{-}03\ \mathrm{m}^3\ \mathrm{s}^{-2}$ as discharge on the inflow boundary. The final time is $T = 38.2$ s. As for the rainfall test case, the final time was chosen such that the outflow discharge at T is approximately equal to the half of the inflow discharge. We show in Figure 6 the side-view of the water height at the final time.

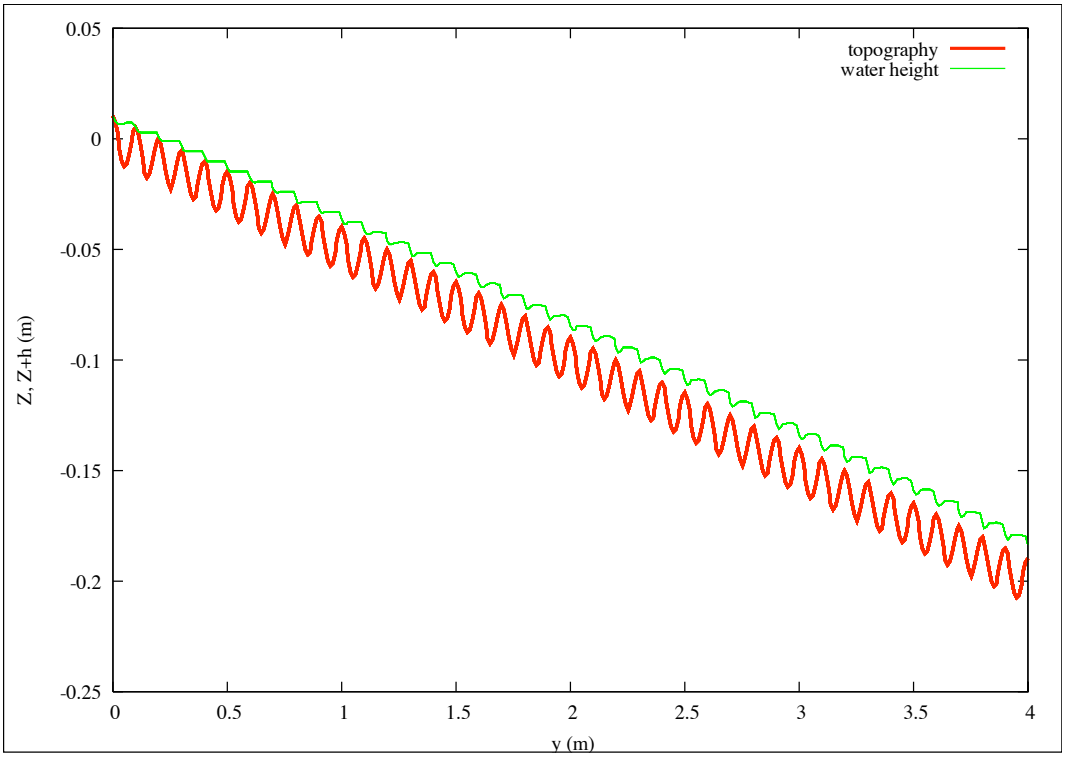

Figure 5: Side-view of the water height at the final time for the rainfall test case

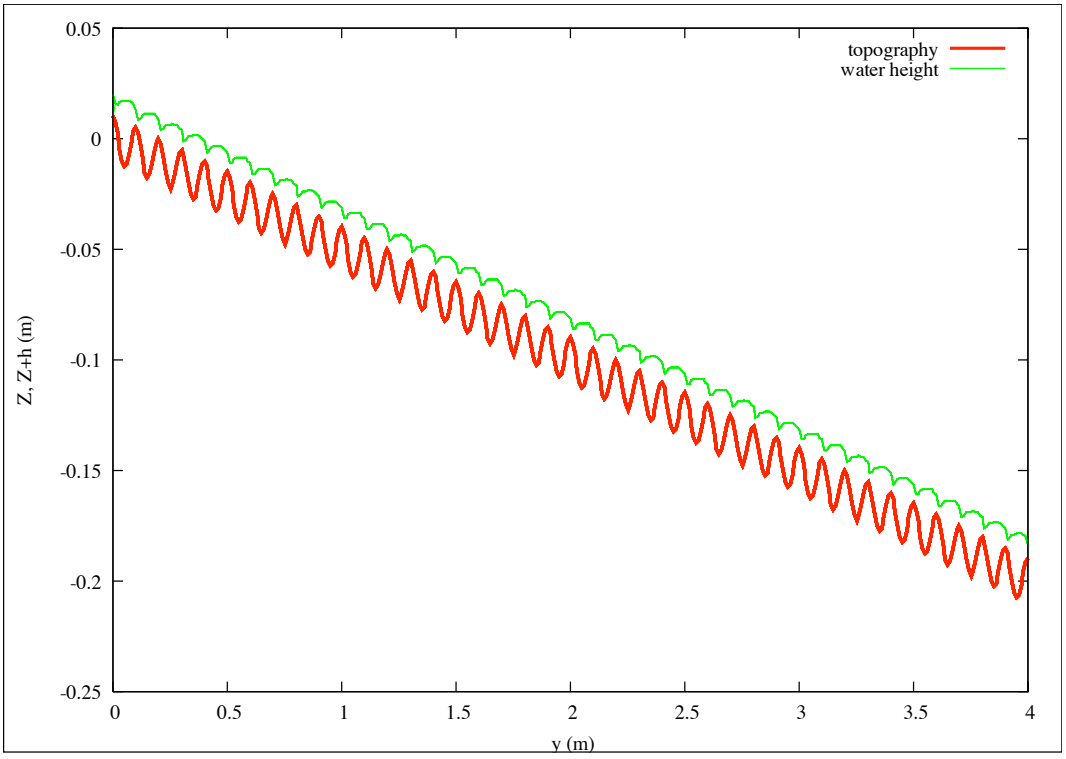

Figure 6: Side-view of the water height at the final time for the inflow test case

3.2 Numerical results on the new model

In this paragraph, we perform numerical tests on the new model (2.3). The furrows are now removed from the topography defined by (3.5). So, it is now reduced to an inclined plane with the same slope:

$$Z(x, y) = -0.05\, y. \tag{3.6}$$

The length of the domain is now discretized with a space step equal to the average wavelength of the furrows which is 0.1 m. We keep the same space step along the width of the domain. Therefore, the domain is discretized by a mesh of 800 rectangles. The initial conditions remain unchanged, i.e. $\boldsymbol{u}(0, \boldsymbol{x}) = \mathbf{0}$ and $h(0, \boldsymbol{x}) = 0$. In order to show the ability of the model (2.3) to take into account the effects of the furrows, we compare the water height and the discharge at the outflow with the reference solutions computed previously. To that end, we first introduce $\overline{h}_i^n$ the average of the reference water height contained in the furrow i at the time t_n, computed in the previous paragraph. We next denote by e^h the effective water height error defined by

$$e^h = \left(\frac{\sum_n \sum_i |\overline{h}_i^n - h_i^n|^2}{\sum_n \sum_i |\overline{h}_i^n - h_i^{0,n}|^2} \right)^{1/2},$$

where h_i^n and $h_i^{0,n}$ are the water heights in the furrow i at time t_n computed with the model (2.3) for given K_0 and C and for $K_0 = 0$, respectively. Finally we denote e^Q the discharge error defined by

$$e^Q = \frac{1}{N} \sum_{n=1}^{N} |Q_n^* - Q_n|,$$

where Q_n^* and Q_n are the reference discharge computed in the previous paragraph and the discharge computed with the model (2.3) respectively. The integer N notes the total number of time steps in the computations.

3.2.1 Rainfall test case

We present, in Figure 7, the water height error e^h as a function of K_0 for the rainfall test case. The value of C is fixed to $C = 10$. We note that the minimum of the error is $e^h \simeq 0.2518$ for $K_0 = 0.02$. Then by optimizing with respect to the two parameters K_0 and C, we finally find the minimum $e^h \simeq 0.1417$ corresponding to $K_0 = 0.02$ and $C = 0.4$. The corresponding discharge error is $e^Q \simeq 2.2356\text{E}{-}05$. We notice that the new model (2.3) allows to diminish the L^2 error on the water height by a factor 7 with respect to the case $K_0 = 0$, showing that the furrow effects are well taken into account.

We now report the results obtained with the two-layer like model (2.4) for this test case. Figure 8 shows the water height error e^h for different Manning's coefficient k. We note

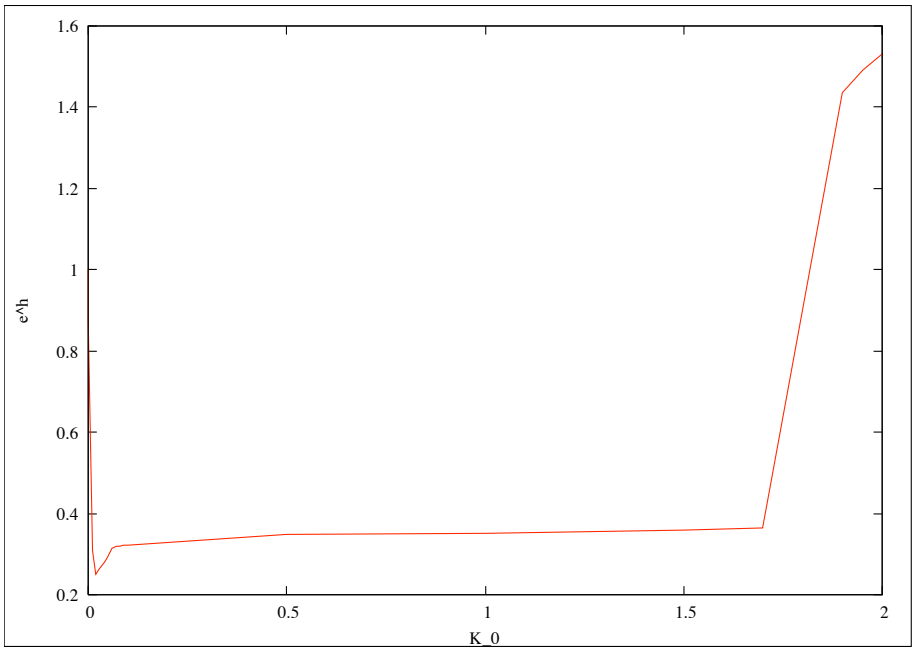

Figure 7: The water height error e^h for the model (2.3) for the rainfall test case

that the minimum is $e^h \simeq 0.0422$ for $k = 0.03$ which is close to the chosen reference coefficient $k = 0.04$. The corresponding discharge error is $e^Q \simeq 1.3179\text{E}{-}05$. We notice that the two-layer model allows to diminish the L^2 error on the water height by a factor 23 with respect to the model (2.3) for the case $K_0 = 0$.

Figure 9 shows the ratio between the outflow discharge and the rain discharge at different times, for the models (2.3) with $K_0 = 0.02$, $C = 0.4$ and $K_0 = 0$ respectively, for the model (2.4) with $k = 0.03$ and for the reference model computed in Paragraph 3.1. We observe that although the domain in the new model is an inclined plane, the additional friction term is able to retain the water for a moment during the rainfall, and so, simulates well the existence of the furrows.

3.2.2 Inflow test case

Figure 10 shows the water height error e^h as a function of K_0 for a fixed value of C to $C = 10$ in the case of the inflow test. We note that the minimum of the error is $e^h \simeq 0.6167$ for $K_0 = 0.005$. The corresponding discharge error is $e^Q \simeq 1.453\text{E}{-}06$. We note that the model (2.3) allows to diminish the L^2 error on the water height by a factor 1.62 with respect to the case K_0. We present in Figure 11 the ratio between the outflow discharge and the imposed inflow discharge at different times, for the models (2.3) with $K_0 = 0.005$, $C = 10$ and $K_0 = 0$ respectively and for the reference model computed in Paragraph 3.1.

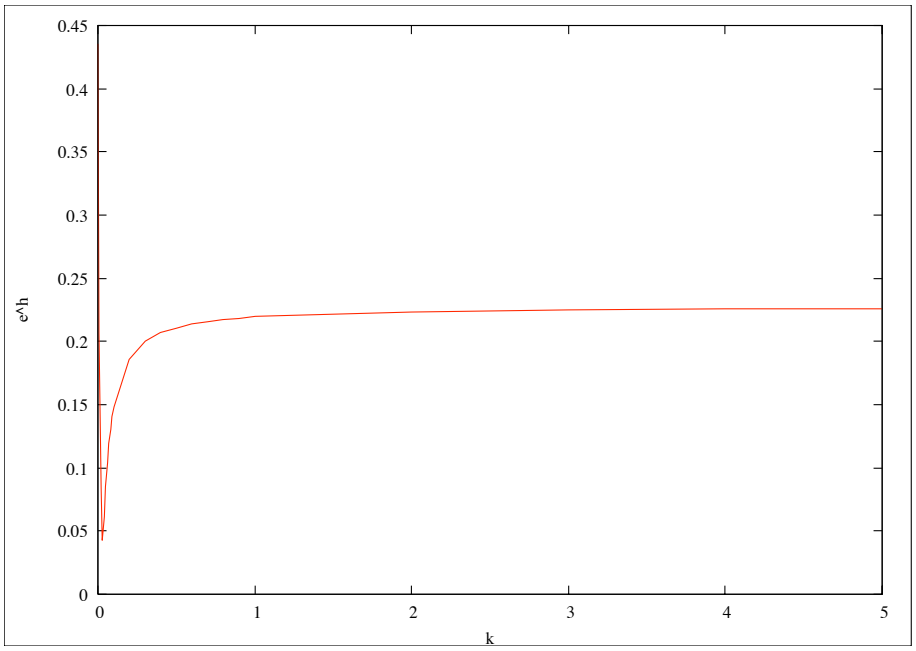

Figure 8: The water height error e^h for the two-layer like model (2.4)

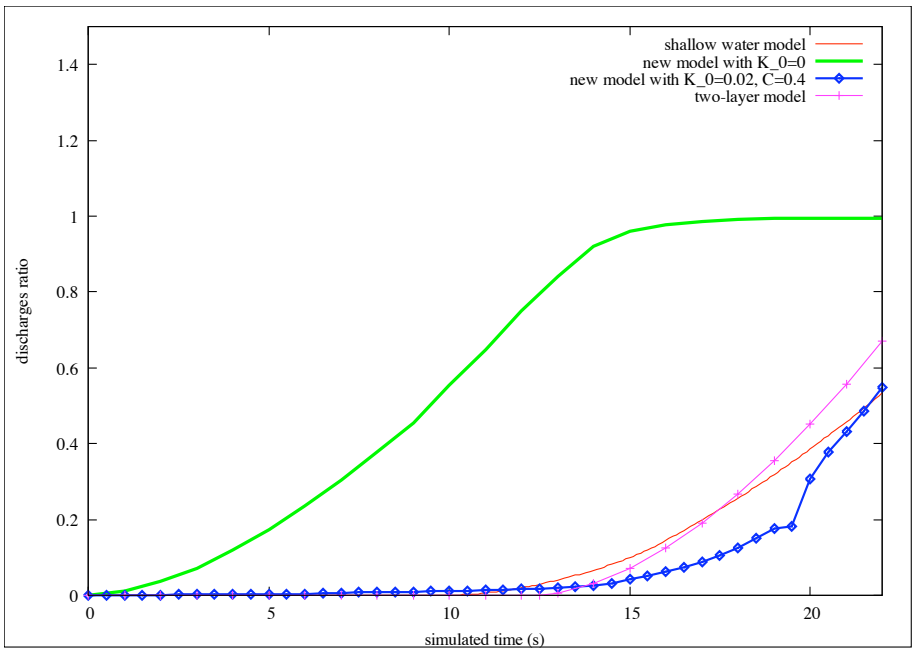

Figure 9: The ratio in time between the outflow discharge and the rain discharge for all the models

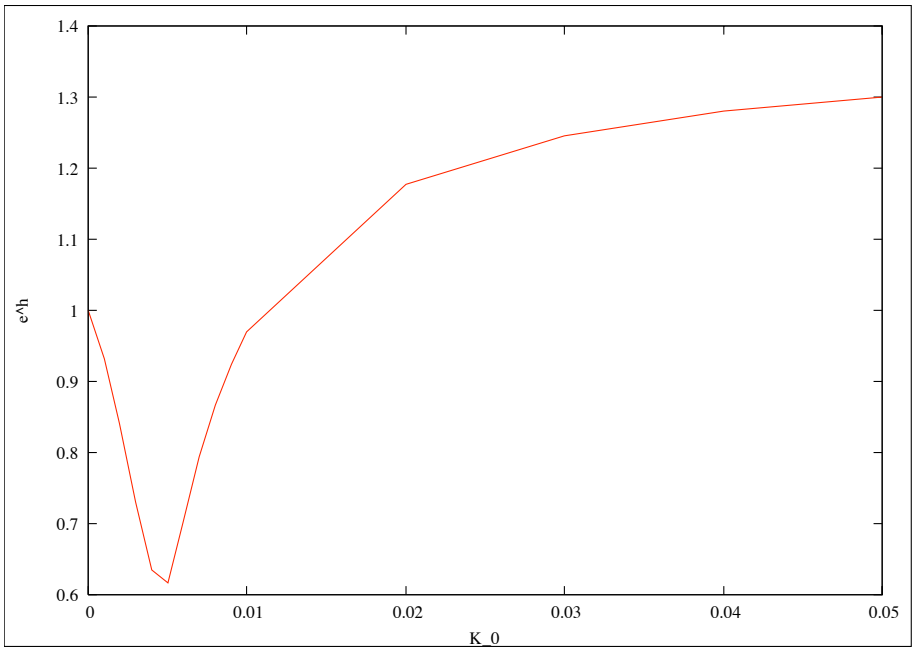

Figure 10: The water height error e^h for the model (2.3) for the inflow test case

We again observe that the new model simulates well the existence of the furrows.

3.2.3 Performance of the new model with calibrated coefficients

In practice, in order to use of the new model (2.3) to describe shallow flows with furrows effects, we need to fix the values of the coefficients K_0 and C. In this paragraph, we only consider the rainfall test cases and we use the calibrated values obtain previously: $K_0 = 0.02$ and $C = 0.4$. Our aim here is to show the performance of the model (2.3) with those values for the coefficients.

We present in Table 1 the errors e^h and e^Q as a function of the space step with respect to the length of the domain. This space step varies from 0.1 m to 0.4 m which allows a cell to contain from 1 to 4 periods of the furrows. We can notice that the variation of the error e^h is small. The motivation of this test is that, for the extension to fully two-dimenional problems, the new model has to predict the flow directions at each grid cell over the area of agricultural fields. As a consequence, the dimension of a grid cell can vary from 1 to 100 m^2. So, a grid cell typically contains several furrows. At the same time, we also present in Table 1 the computational times to compute the solutions of the new model as a function of the space step. The values are normalized with respect to the computational time to compute the reference solutions. As we can observe the new model allows to reduce the computational time for at least 90% and can easily achieve a 97% decrease in the computational type.

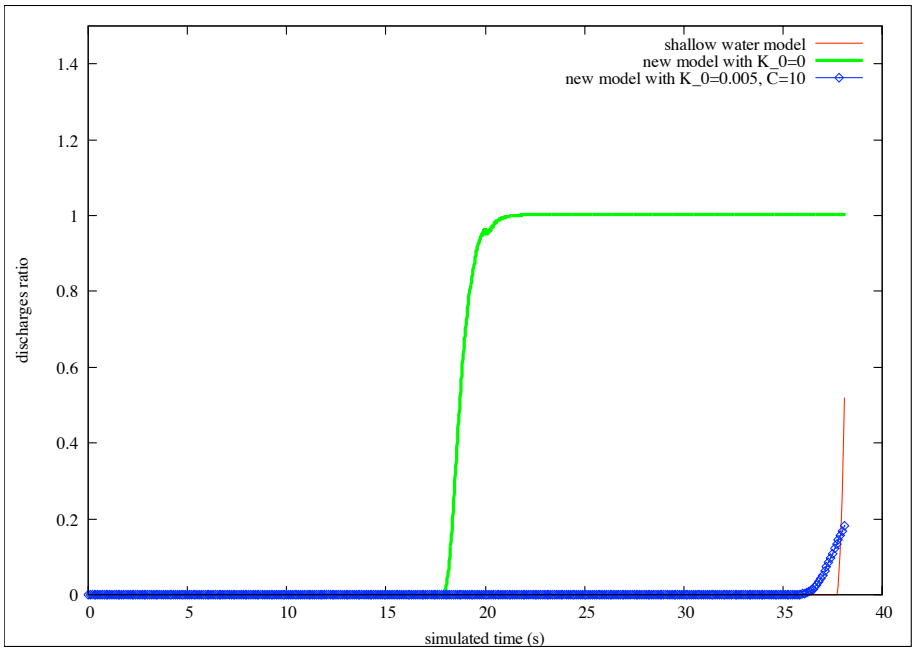

Figure 11: The ratio in time between the outflow discharge and the imposed inflow discharge for all the models

Space step with respect to the y-axis	e^h	e^Q	CPU time
0.1	0.1417	$2.2356\,E-05$	0.11
0.2	0.2244	$5.1038\,E-05$	0.0574
0.4	0.2616	$5.3693\,E-05$	0.0255

Table 1: Water height errors, flowrate errors and CPU times (normalized with respect to the time to compute the reference solution).

In Table 2, we present for different slopes of the topography (with realistic values in reference to agricultural fields), the errors e^h and e^Q for the calibrated values $K_0 = 0.02$ and $C = 0.4$. We note that the new model allows to reduce the L^2 error on the water height by at least a factor 4 showing that the effects of the furrows are well taken into account. Compared with Table 3, where for each slope, the minimum of the error e^h is computed and where the corresponding coefficients K_0, C and error e^Q are presented, we see that the new model with the calibrated values $K_0 = 0.02$, $C = 0.4$ still yields accurate results.

Table 4 shows, for different Manning's coefficients and for a slope kept at 5%, the errors e^h and e^Q for the calibrated values $K_0 = 0.02$ and $C = 0.4$. Compared with Table 5, where for each Manning coefficient, the minimum of the error e^h is computed and where the corresponding coefficients K_0, C and error e^Q are presented, we see that the new model

with the calibrated values also yields accurate results.

The last results that we present are dedicated to water heights and discharges errors at steady state for the shallow water model (2.1). The final time of the simulations is now $T = 50$ s. Figure 12 shows the ratio between the rain discharge and the outflow discharge at different times, for the new model with the calibrated coefficients and for the shallow water model (2.1) where the furrows is known explicitly. We now denote e_s^h the water height error at steady state defined by

$$e_s^h = \left(\sum_i |\overline{h}_i - h_i|^2 \right)^{1/2}$$

where $\overline{h}_i^n$ is the average water height contained in the furrow i computed with the shallow water model (2.1) and h_i is the water height in the furrow i computed with the new model. We note that here this error is $e_s^h \simeq 5.468\text{E}{-}02$. Next we denote e_s^Q the discharge error at steady state defined by

$$e_s^Q = |Q^* - Q|$$

where Q^* and Q are the discharges computed with the shallow water model (2.1) and the new model respectively. We note that here this error is $e_s^Q \simeq 3.63\text{E}{-}05$. We thus deduce that at steady state, the new model with the calibrated coefficients takes well into account the effects of the furrows and approximates well the shallow water model (2.1).

slope	K_0	C	e^h	e^Q
2%	0.02	0.4	0.2434	$7.3656\,E-05$
5%	0.02	0.4	0.1417	2.22335E−05
8%	0.02	0.4	0.2194	$1.3578\,E-04$
11%	0.02	0.4	0.2035	$1.2817\,E-04$

Table 2: The errors e^h and e^Q for different slopes of the topography with $K_0 = 0.02$ and $C = 0.4$

slope	K_0	C	e^h	e^Q
2%	0.02	0.3	0.2167	2.26E−05
5%	0.02	0.4	0.1417	2.22335E−05
8%	0.04	0.4	0.1205	6.453E−05
11%	0.04	0.4	0.1089	5.3334E−05

Table 3: The minimum errors e^h and e^Q with the corresponding coefficients K_0 and C for different slopes of the domain

4 Conclusions

In this paper, we have proposed a new shallow water model (2.3) in order to describe the effects of furrows during overland flow without representing them explicitly. The main idea is to include in the classical shallow water equations the additional friction term (2.2) that takes into account the effects of these furrows. The new model was proposed under the assumptions that the direction of the flow is fluvial and is parallel to the length of the domain. We have also assume that there is no infiltration and no soil erosion.

We have presented numerical results to show the efficiency and the performance of the new model. In particular, we show that the new model with calibrated coefficients does not depend on the slope of the domain (see Tab. 2 and Tab. 3) and does not depend on the soil friction coefficient (see Tab. 4 and Tab. 5).

The numerical results presented in this paper are encouraging and indicate that the idea could be extended to more complex two-dimensional flows. This is now the main goal of the forthcoming works. Note that, unlike the two-layer model (2.4), the new model (2.3) can easily be generalized to two-dimensional problems. These extensions include the random variations of the height of the furrows. As we have already mentioned in Remark

Manning's coefficient	K_0	C	e^h	e^Q
0.001 $\mathrm{m}^{\frac{1}{3}}\ \mathrm{s}^{-1}$	0.02	0.4	0.0744	$9.6729\,E-05$
0.04 $\mathrm{m}^{\frac{1}{3}}\ \mathrm{s}^{-1}$	0.02	0.4	0.1417	$2.2356\,E-05$
0.1 $\mathrm{m}^{\frac{1}{3}}\ \mathrm{s}^{-1}$	0.02	0.4	0.2746	$1.369\,E-04$

Table 4: The errors e^h and e^Q for $K_0 = 0.02$ and $C = 0.4$ for different Manning's coefficient

Manning's coefficient	K_0	C	e^h	e^Q
0.001 $\mathrm{m}^{\frac{1}{3}}\ \mathrm{s}^{-1}$	0.02	0.4	0.0744	$9.6729\,E-05$
0.04 $\mathrm{m}^{\frac{1}{3}}\ \mathrm{s}^{-1}$	0.02	0.4	0.1417	$2.2356\,E-05$
0.1 $\mathrm{m}^{\frac{1}{3}}\ \mathrm{s}^{-1}$	0.02	0.5	0.265	$1.2155\,E-04$

Table 5: The minimum errors e^h and e^Q with the corresponding coefficients K_0 and C for different Manning's coefficient

2.1, these variations can be taken into account in the constant C of the additional friction term defined in (2.2). The extensions also include the direction of the furrows which is not perpandicular to the slope of the domain in order to study the effects of this direction with respect to the slope. This direction can be taken into account by a rotation of the model (2.3).

Acknowledgements

This work was supported by the ANR project METHODE #ANR-07-BLAN-0232 (`http://www.univ-orleans.fr/mapmo/methode/`) and the Région Centre, France. The authors wish to thank all the members of the project for fruitful discussions and for many helpful comments.

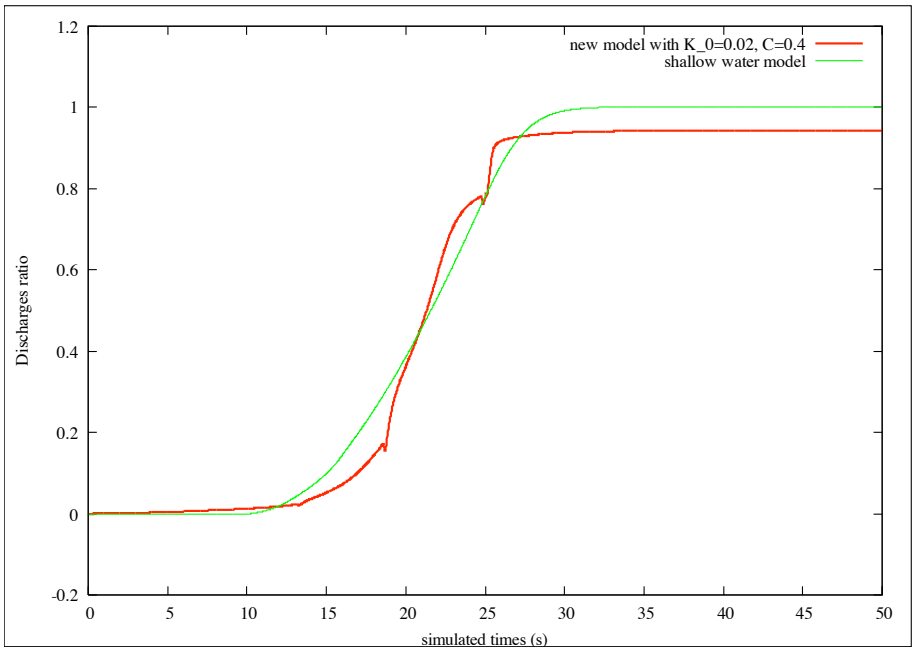

Figure 12: The discharges ratio at steady state

References

[1] E. Audusse. A multilayer Saint-Venant model: derivation and numerical validation. *Discrete Contin. Dyn. Syst. Ser. B*, **5**(2):189–214, 2005.

[2] E. Audusse, F. Bouchut, M.-O. Bristeau, R. Klein, and B. Perthame. A fast and stable well-balanced scheme with hydrostatic reconstruction for shallow water flows. *SIAM J. Sci. Comput.*, **25**(6):2050–2065, 2004.

[3] E. Audusse and M.-O. Bristeau. Finite-volume solvers for a multilayer Saint-Venant system. *Int. J. Appl. Math. Comput. Sci.*, **17**(3):311–319, 2007.

[4] K. Beven. On undermining the science? *Hydrol. Process.*, **20**:2050–2065, 2006.

[5] F. Bouchut. *Nonlinear stability of finite volume methods for hyperbolic conservation laws and well-balanced schemes for sources.* Frontiers in Mathematics. Birkhäuser Verlag, Basel, 2004.

[6] M.-O. Bristeau and B. Coussin. Boundary conditions for the shallow water equations solved by kinetics schemes. *Inria report*, RR-4282, 2001.

[7] M. Castro, J. Macías, and C. Parés. A Q-scheme for a class of systems of coupled conservation laws with source term. Application to a two-layer 1-D shallow water system. *M2AN Math. Model. Numer. Anal.*, **35**(1):107–127, 2001.

[8] F. Darboux, P. Davy, and C. Gascuel-Odoux. Effect of depression storage capacity on overland-flow generation for rough horizontal surfaces: Water transfer distance and scalling. *Earth Surf. Process. Landforms*, **27**(2):177–191, 2002.

[9] A.J.C de Saint-Venant. Théorie du mouvement non-permanent des eaux, avec application aux crues des rivières et à l'introduction des marées dans leur lit. *C. R. Math. Acad. Sci. Paris*, **73**:147–154, 1871.

[10] O. Delestre, S. Cordier, F. James, and F. Darboux. Simulation of rain-water overland-flow. In *Proceedings of Symposia in Applied Mathematics, to appear, preprint available at http://hal.archives-ouvertes.fr/hal-00343721/fr/.* 2009.

[11] O. Delestre and F. James. Simulation of rainfall events and overland flow. In *Monografías Matemáticas García de Galdeano, to appear, preprint availabe at http://hal.archives-ouvertes.fr/hal-00426694/fr/.* 2009.

[12] S. Ferrari and F. Saleri. A new two-dimensional shallow water model including pressure effects and slow varying bottom topography. *M2AN Math. Model. Numer. Anal.*, **38**(2):211–234, 2004.

[13] J.-F. Gerbeau and B. Perthame. Derivation of viscous Saint-Venant system for laminar shallow water; numerical validation. *Discrete Contin. Dyn. Syst. Ser. B*, **1**(1):89–102, 2001.

[14] J. E. Gilley, D. C. Flanagan, E. R. Kottwitz, and M. A. Weltz. Darcy-weisbach roughness coefficients for overland flow. pages 25–52. Parsons AJ & Abrahams AD (ed.), University College London Press, 1992.

[15] V. Jetten, A. de Roo, and D. Favis-Mortlock. Evaluation of field-scale and catchment-scale soil erosion models. *Catena*, **37**:521–541, 1999.

[16] V. Jetten, G. Govers, and R. Hessel. Erosion models: quality of spacial predictions. *Hydrol. Process.*, **17**:887–900, 2003.

[17] C. X. Jin, M. J. M. Römkens, and F. Griffioen. Estimating manning's roughness coefficient for shallow overland flow in non-submerged vegetative filter strips. *Trans. ASAE*, **43**:1459–1466, 2000.

[18] J. Lhomme. *Modélisation des inondations en milieu urbain : approches unidimensionnelle, bidimensionnelle et macroscopique*. PhD thesis, Université Montpellier II, 2006.

[19] F. Marche. Derivation of a new two-dimensional viscous shallow water model with varying topography, bottom friction and capillary effects. *Eur. J. Mech. B Fluids*, **26**(1):49–63, 2007.

[20] O. Planchon, M. Esteves, N. Silvera, and J. Lapetite. Microrelief induced by tillage: measurement and modelling of Surface Storage Capicity. *Catena*, **46**:141–157, 2001.

[21] P. Quinn, K. Beven, P. Chevallier, and O. Planchon. The prediction of hillslope flow paths for distributed hydrological modelling using digital terrain models. *Hydrol. Process.*, **5**:59–79, 1991.

[22] V. Souchère, D. King, J. Darousin, F. Papy, and A. Capillon. Effects of tillage on runoff directions: consequences on runoff contributing areas within agricultural catchments. *J. Hydrol.*, **206**:256–267, 1998.

[23] I. Takken, G. Govers, V. Jetten, L. Nachtergaele, A. Steegen, and J. Poesen. Effect of tillage and runoff and erosion patterns. *Soil Tillage Res.*, **61**:55–60, 2001.

[24] D. G. Tarboton. A new method for the determination of flow directions and upslope areas in grid digital elevation models. *Water Resour. Res.*, **33**:309–331, 1997.